J|A|C|S
ARTICLES
Published on Web 02/11/2006

Barriers of Hydrogen Abstraction vs Halogen Exchange: An Experimental Manifestation of Charge-Shift Bonding

Philippe C. Hiberty,*,† Claire Megret,† Lingchun Song,‡ Wei Wu,*,‡ and Sason Shaik*,§

Contribution from the Laboratoire de Chimie Physique, Groupe de Chimie Théorique, Université de Paris-Sud, 91405 Orsay Cédex, France, the Department of Chemistry and State Key Laboratory for Physical Chemistry of Solid Surfaces, Xiamen University, Xiamen, Fujian 361005, P.R. of China, and the Department of Organic Chemistry and the Lise-Minerva Center for Computational Chemistry, The Hebrew University, Jerusalem 91904, Israel

Received May 13, 2005; E-mail: philippe.hiberty@lcp.u-psud.fr; weiwu@xmu.edu.cn; sason@yfaat.ch.huji.ac.il

Abstract: This paper shows that the differences between the barriers of the halogen exchange reactions, in the H + XH systems, and the hydrogen abstraction reactions, in the X + HX systems (X = F, Cl, Br), *measure the covalent−ionic resonance energies of the corresponding X−H bonds*. These processes are investigated using CCSD(T) calculations as well as the breathing-orbital valence bond (BOVB) method. Thus, the VB analysis shows that (i) at the level of covalent structures the barriers are the same for the two series and (ii) the higher barriers for halogen exchange processes originate solely from the less efficient mixing of the ionic structures into the respective covalent structures. The barrier differences, in the HXH vs XHX series, which decrease as X is varied from F to I, *can be estimated as one-quarter of the covalent−ionic resonance energy of the H−X bond*. The largest difference (22 kcal/mol) is calculated for X = F in accord with the finding that the H−F bond possesses the largest covalent−ionic resonance energy, 87 kcal/mol, which constitutes the major part of the bonding energy. The H−F bond belongs to the class of "charge-shift" bonds (Shaik, S.; Danovich, D.; Silvi, B.; Lauvergnat, D. L.; Hiberty, P. C. *Chem. Eur. J.* **2005**, *21*, 6358), which are all typified by dominant covalent−ionic resonance energies. Since the barrier difference between the two series is an experimental measure of the resonance energy quantity, in the particular case of X = F, the *unusually high barrier* for the fluorine exchange reaction emerges as an experimental manifestation of charge-shift bonding.

I. Introduction

In 1975 Schaefer and co-workers published a series of pioneering high-level configuration interaction (CI) calculations on the hydrogen transfer reaction between fluorine atoms (reaction 1, X = F) and the fluorine exchange reaction (reaction 2, X = F).[1]

$$X^{\bullet} + H{-}X' \rightarrow X{-}H + X'^{\bullet} \quad (X = F,Cl, Br, I) \qquad (1)$$

$$H^{\bullet} + X{-}H' \rightarrow H{-}X + H'^{\bullet} \quad (X = F,Cl, Br, I) \qquad (2)$$

In challenge of most contemporary semiempirical results, which predicted very low barriers[2] (with one exception[3]), Schaefer et al. predicted that the barrier for HFH is 42−49 kcal/mol, while this for the FHF system is 22−24 kcal/mol. This large difference in the barrier of the two reactions is still an intriguing theoretical prediction. Indeed, 3 years later Polanyi et al. tested and verified this prediction by experimental means, using the reactions of HF with D. Thus, the very endothermic reaction channel of hydrogen abstraction leading to F + H_2 was found to have a barrier of only 34.2 kcal/mol,[4] compared with the thermoneutral F-abstraction reaction that possessed a significantly larger barrier.[5] The conclusion of Polanyi et al.[5] stated as follows: "This high activation barrier for a thermoneutral reaction is surprising, as is the fact that the thermoneutral reaction path has a barrier substantially in excess of the endothermic reaction path", reflects the intriguing aspect in these findings.[5] The prediction and its experimental verification was a victory for quantum chemistry, but it also constitutes a fundamental and still unresolved problem: Where does the high HFH barrier come from? As shall be seen, the solution of this puzzle will provide the first experimental evidence for the type of electron pair bonding, so-called "charge-shift bonding" (CS-bonding), which derives from large resonance energies between covalent and ionic structures, in the language of valence bond (VB)

† Université de Paris-Sud.
‡ Xiamen University.
§ The Hebrew University.

(1) (a) Bender, C. F.; Garrison, B. J.; Schaefer, H. F. *J. Chem. Phys.* **1975**, *62*, 1188. (b) O'Neil, S. V.; Schaefer, H. F.; Bender, C. F. *Proc. Natl. Acad. Sci. U.S.A.* **1974**, *71*, 104. (c) Bender, C. F.; O'Neil, S. V.; Pearson, P. K.; Schaefer, H. F. *Science* **1972**, *176*, 1412. (d) Bender, C. F.; Bauschlicher, C. W.; Schaefer, H. F. *J. Chem. Phys.* **1974**, *60*, 3707.
(2) (a) Muckerman, J. T. *J. Chem. Phys.* **1971**, 54, 1155. (b) Muckerman, J. T. *J. Chem. Phys.* **1972**, *56*, 2997. (c) Wilkins, R. L. *J. Chem. Phys.* **1972**, *57*, 912. (d) Blais, N. C.; Truhlar, D. G. *J. Chem. Phys.* **1973**, *58*, 1090. (e) Tully, J. C. *J. Chem. Phys.* **1973**, *58*, 1396.
(3) Thompson, D. L. *J. Chem. Phys.* **1972**, *57*, 4170.
(4) Peterson, K. A. *J. Phys. Chem. A* **1997**, *101*, 6280.
(5) Bartoszek, F. E.; Manos, D. M.; Polanyi, J. C. *J. Chem. Phys.* **1978**, *69*, 933.

 10.1021/ja053130m CCC: $33.50

theory.[6] CS-bonding has recently been revealed by two independent theoretical methods, valence bond (VB) and electron-localization functions (ELF).[7]

It turns out that the HFH vs FHF puzzle is part of a general trend that is found when one compares the barriers of the identity reactions 1 and 2. Thus, at a consistent level of theory, RCCSD(T)//6-31++G*, the barriers for the collinear reaction 1 are 22.2, 15.6, and 11.3 kcal/mol for X = F, Cl, and Br, respectively.[8] For the IHI system, molecular dynamic calculations are usually done on DIM[9] or LEPS[10] surfaces, which display a barrier of 3 kcal/mol or less. Use of larger basis sets lowers the calculated barriers, but the tendency remains the same (see below). The ClHCl system has been much studied at the ab initio level.[11−18] A recent accurate ab initio calculation by Schatz et al.,[17] at the level of RCCSD(T) with an augmented triple-ζ basis set, reports a barrier of 10.1 kcal/mol for a bent transition state, the collinear transition state lying only 1.3 kcal/mol higher. Another accurate calculation has been reported by Fox and Schlegel for the FHF system, yielding a barrier of 17.5 kcal/mol for reaction 1 via a bent transition state.[12] Recent RCCSD(T)/6-311++G(3df,3pd) calculations led to a barrier of 17.8 kcal/mol (FHF angle = 132.6°). At the same level, the barrier for a constrained linear TS was 20.9 kcal/mol.[18] From these studies, it appears that collinear transition states are not much higher in energy than the respective bent structures and that the activation barrier for the hydrogen exchange reaction 1 is close to 20 kcal/mol for X = F, and gradually diminishes in the series from X = F to I.

Consider now the halogen exchange series in reaction 2 for X = F−I. At a consistent theoretical level, QCISD(T), and with a rather large basis set, the barriers for the HXH system are 42.7, 20.2, 13.8, and 6.4 kcal/mol for X = F, Cl, Br, and I, respectively.[19] More recent calculations confirm these values. Accurate computations converge to a barrier of ca. 12 kcal/mol for the HBrH system,[20,21] 18 kcal/mol for HClH,[4,22,23] and 41 kcal/mol for HFH.[24] All the transition states are found to be linear. Within this series, too, the barriers decrease as the X−H bond energies decrease. Despite the existence of the same trends in the two series, it is apparent that for the same bond strength, the barriers in reaction 2 are consistently higher than those in reaction 1.

According to a recent valence bond (VB) modeling of the hydrogen transfer process,[8,25,26] the identity barrier of linear reactions is gauged primarily by the H−X bond energy, and hence, it is understandable that barriers for reaction 1 are found to decrease in the series from F toward I.[9,27] Furthermore, these trends are consistent with an activation barrier of ca. 10 kcal/mol for the $H' + H_2 \rightarrow HH' + H$ reaction, since the Cl−H and H−H bond strengths are approximately the same, while the stronger F−H bond leads to a higher barrier and the weaker Br−H and I−H bonds produce lower barriers for reaction 1. The VB model explains also the decrease of the barrier in the series of reaction 2, since the X−H bond strength decreases as X changes from F gradually to I. However, the model as such does not explain the consistently higher barriers for the halogen exchange (reaction 2) compared with the hydrogen exchange (reaction 1). Importantly, the model does not account for the fact that the barrier differences (reaction 1 vs reaction 2) decrease from X = F, where the difference is ca. 20 kcal/mol, to X = I, where the difference is ca. 3 kcal/mol.

Where does the higher barrier for the HXH systems come from, and why is it particularly high for X = F? A tentative explanation has been proposed,[19,28,29] in terms of Pauli repulsion between the attacking hydrogen in reaction 1 and the doubly occupied *n*s orbital of the central halogen atom. While this proposal might seem reasonable, it still has to be numerically tested. Furthermore, the same repulsion should be encountered in the FHF transition state, but nevertheless the corresponding barrier is for some reason rather small. These puzzles will be investigated here by means of modern VB calculations of the barriers for reactions 1 and 2, for X = F, Cl, and Br, followed by qualitative VB modeling of the results.

The paper is organized as follows: A qualitative analysis of reactions 1 and 2, in terms of VB diagrams will first be provided in the next section. Subsequently, the concept of CS-bonding, which occurs in bonds with very large covalent−ionic resonance energies,[6] will be briefly reviewed, and the theoretical methods and computational results will be presented in the following sections.

2. A Qualitative Valence Bond Analysis

According to VB theory, a hydrogen halide is described as a resonating combination of two principal VB structures, a covalent one, hereafter designated as X•−•H, and an ionic one, X^-H^+, for an electronegative X group. The second ionic structure X^+H^-, is expected to be unimportant and is neglected hereafter for the sake of simplicity. Mixing the remaining two VB structures to generate the ground state brings some covalent−ionic "resonance energy" RE_{C-I}; this is a stabilizing quantity that will play a primary role in the following discussion.

Extending the VB description to the above reactions, the ground potential energy surface of reaction 1 can be calculated,

(6) (a) Sini, G.; Maitre, P.; Hiberty, P. C.; Shaik, S. S. *J. Mol. Struct. (THEOCHEM)* **1991**, *229*, 163. (b) Shaik, S.; Maitre, P.; Sini, G.; Hiberty, P. C. *J. Am. Chem. Soc.* **1992,** *114*, 7861. (c) Lauvergnat, D. L.; Hiberty, P. C.; Danovich, D.; Shaik, S. *J. Phys. Chem.* **1996,** *100,* 5715. (d Shurki, A.; Hiberty, P. C.; Shaik, S. *J. Am. Chem. Soc.* **1999**, *121*, 822. (e) Galbraith, J. M.; Blank, E.; Shaik, S.; Hiberty, P. C. *Chem. Eur. J.* **2000**, *6*, 2425. (f) Lauvergnat, D. L.; Hiberty, P. C. *J. Mol. Struct. (THEOCHEM)* **1995**, *338*, 283.
(7) Shaik, S.; Danovich, D.; Silvi, B.; Lauvergnat, D. L.; Hiberty, P. C., *Chem. Eur. J.* **2005**, *21*, 6358.
(8) Shaik, S.; Wu, W.; Dong, K.; Song, L.; Hiberty, P. C. *J. Phys. Chem. A* **2001**, *105*, 8226.
(9) Last, I.; Baer, M. *J. Chem. Phys.* **1984**, *80*, 3246.
(10) Manz, J.; Romelt, J. *Chem. Phys. Lett.* **1981**, *81*, 179.
(11) Vincent, M. A.; Connor, J. M. L.; Besley, N. A.; Knowles, P. J.; Schatz, G. C.*Chem. Phys. Lett.* **1993**, *203*, 415.
(12) Fox, G. L.; Schlegel, H. B. *J. Am. Chem. Soc.* **1993**, *115*, 6870.
(13) Malcom, N. O. J.; McDouall, J. J. W. *J. Phys. Chem.* **1994**, *98*, 12579.
(14) Visscher, L.; Dyall, K. G. *Chem. Phys. Lett.* **1995**, *239*, 181.
(15) Maierle, C. S.; Schatz, G. C.; Gordon, M. S.; McCabe, P.; Connor, J. N. L. *J. Chem. Soc., Faraday Trans.* **1997**, *93*, 709 and references therein.
(16) Gonzalez, M.; Hijazo, J. Novoa, J. J.; Sayos, R. *J. Chem. Phys.* **1998**, *108*, 3168.
(17) Dobbyn, A. J.; Connor, J. N. L.; Besley, N. A.; Knowles, P. J.; Schatz, G. C. *Phys. Chem. Chem. Phys.* **1999**, *1*, 957.
(18) Shaik, S.; de Visser, S. P.; Wu, W.; Song, L.; Hiberty, P. C. *J. Phys. Chem. A* **2002**, *106*, 5043.
(19) Dobbs, K. D.; Dixon, D. A. *J. Phys. Chem.* **1993**, *97*, 2085.
(20) Kurosaki, Y.; Takayanagi, T. *J. Chem. Phys.* **2003**, *119*, 7838
(21) Lynch, G. C.; Truhlar, D. G.; Brown, F. B.; Zhao, J.-G. *J. Phys. Chem.* **1995**, *99*, 207.
(22) Bian, W.; Werner H.-J. *J. Chem. Phys.* **2000**, *112*, 220.
(23) Schwneke, D. W.; Tucker, S. C.; Steckler, R.; Brown, F. B.; Lynch, G. C.; Truhlar, D. G. *J. Chem. Phys.* **1989**, *90*, 3110.
(24) Stark, K.; Werner, H. J. *J. Chem. Phys.* **1996**, *104*, 6515.
(25) Song, L.; Wu, W.; Dong, K.; Hiberty, P. C.; Shaik, S. *J. Phys. Chem. A* **2002**, *106*, 11361.
(26) Su, P.; Song, L.; Wu, W.; Hiberty, P. C.; Shaik, S. *J. Am. Chem. Soc.* **2004**, *126*, 13539.
(27) Parr, C. A.; Truhlar, D. G. *J. Phys. Chem.* **1971**, *75*, 1844.
(28) Wadt, W. R.; Winter, N. W. *J. Chem. Phys.* **1977**, *67*, 3068.
(29) Dunning, T. H., Jr. *J. Phys. Chem.* **1984**, *88*, 2469.

Scheme 1

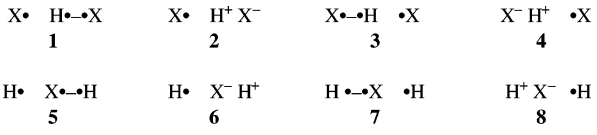

at any geometry, as a resonating mixture of the VB structures **1**−**4** (see Scheme 1), the reactants being described as the combination **1** ↔ **2**, and the products as **3** ↔ **4**.

Similarly, in reaction 2, **5** ↔ **6** and **7** ↔ **8** correspond, respectively, to the reactants and products, and the whole potential surface is generated by the optimized combination of the VB structures **5**−**8**.

A "VB configuration mixing diagram" (VBCMD) is obtained when, in addition to the ground-state reaction profile, the effective VB structures of a chemical reaction are traced *individually* along a reaction coordinate. Such diabatic curves cross in the region of the transition state, and the reaction barrier arises from avoided crossing of these curves to generate the adiabatic ground-state reaction profile. The VB diagram model has been reviewed recently[30] and shown to bring significant insight into the mechanism of barrier formation in chemical reactions. Thus, in the VBCMDs depicted in Figure 1, the energy variations of the covalent structures are plotted as full thin lines, while those of the ionic structures are shown by dotted lines (the diabatic covalent and ionic curves are schematically represented as straight lines but may actually take different shapes). The ground-state reaction profile, resulting from the optimized mixture of all four VB structures, is represented as a bold curve that displays a barrier $\Delta E^{\ddagger}$ at the transition-state geometry.

The advantage of plotting separately the covalent and ionic structures is that this permits a direct appreciation of bond ionicity in the transition state, also called "polar effect", which is considered to be important in hydrogen abstraction reactions.[31] Thus, one may first study the reactions at the purely covalent level, i.e., by omitting the ionic structures (**2**, **4** or **6**, **8**) from Figure 1. One will then get a "covalent reaction profile" Ψ_{cov} (not shown in the diagram) and a covalent barrier $\Delta E^{\ddagger}_{cov}$. Subsequently, the accurate reaction profile will be obtained by allowing the ionic structures to mix with the covalent structures, yielding the actual barrier $\Delta E^{\ddagger}$. At any point of the reaction coordinate, the covalent−ionic resonance energy RE_{C-I} will be defined as the difference between the energy of Ψ_{cov} and the energy of the true ground state. The covalent−ionic resonance energies will of course take different values in the transition state and in the reactants, and the difference ΔRE_{C-I} will correspond to the difference between $\Delta E^{\ddagger}_{cov}$ and $\Delta E^{\ddagger}$, as expressed in eq 3.

$$\Delta RE_{C-I} = \Delta E^{\ddagger}_{cov} - \Delta E^{\ddagger} \qquad (3)$$

This difference between the covalent barrier and the accurate one will thus provide quantitative information about the effect of bond ionicity on reactivity.

Let us first consider reaction 1 at the covalent level. When moving from the geometry of the reactants to the transition state's geometry, structure **1** rises in energy, in Figure 1a, for two reasons: (i) the X•−•H bond is stretched, and (ii) some Pauli repulsion builds up when the attacking X• atom approaches the bound H•. Structure **3** also rises in energy as we move from the product's geometry to the transition state's; at the latter geometry **3** undergoes the same X•−•H stretching and Pauli repulsions and becomes degenerate with **1** at the crossing point, E_c^{cov}. These repulsive three-electron interactions are depicted in Figure 2a for structure **1** (the π lone pairs of the halogen atom are omitted). As can be seen, structure **1** suffers two three-electron repulsive interactions, involving the 1s(H) orbital of the central hydrogen and the *n*s(X) orbitals of both halogen atoms.

Let us now turn to reaction 2. At the transition-state geometry, the degenerate covalent structures **5** and **7** are subject also to the three-electron repulsions, which are illustrated in Figure 2b for **5**. As in the preceding case, these covalent structures are destabilized by X•−•H stretching and two 1s(H)−*n*s(X) three-electron repulsions, i.e., exactly the same factors as in reaction 1. It follows that the shapes of the covalent curves and the height of their crossing point (E_c^{cov} in Figure 1) should, in principle, be the same in both reactions 1 and 2. As a consequence, the covalent ground-state curves, which result from avoided crossing of these covalent curves, should have nearly the same energy profiles in both reactions. Thus, VB theory predicts that, *at the purely covalent level, reactions 1 and 2 should have nearly the same barrier*s. At this level of thinking, we have neglected a possible hybridization of the "*n*s" halogen lone pairs in a direction opposite to the X−H bonding region. Such an effect, if important, would indeed destabilize the HXH transition state with respect to the XHX one and would possibly account for the observed barrier differences, as suggested before.[28,29] Thus, if the hybridization effect is important, it would manifest itself at the covalent level, and lead to higher covalent barriers for HXH than for XHX systems. This will be numerically tested by ab initio VB calculations below.

How do the inclusions of ionic structures modify the simple picture of the covalent-only curves? Let us first consider the halogen exchange, reaction 2. At the transition state's geometry, each ionic structure **6** or **8** undergoes some significant Pauli repulsions, shown in Figure 2d for **6**: one between the 1s(H) orbital of the attacking hydrogen and the *n*s(X) orbital of the halogen and, more importantly, another one between 1s(H) and the np_z(X) orbital. On the other hand, no such repulsions take place in the ionic structures, **2** and **4**, that correspond to reaction 1, since the central moiety, an H^+ cation, is devoid of electrons (Figure 2c). It follows therefore that the crossing point of ionic structures (E_c^{ion} in Figure 1b) for reaction 2 should be much higher than the corresponding E_c^{ion} point in Figure 1a for reaction 1. This in turn leads to a greater loss of transition-state resonance energy RE_{C-I} in reaction 2 compared with that in reaction 2. Consequently, VB theory predicts that the barriers of hydrogen abstractions (1) should be systematically lower than those of the corresponding halogen exchange processes (2), solely due to the trends in the covalent−ionic resonance energy in the transition states for the two reaction families. Of course, the magnitude of this barrier differentiation depends on the importance of the resonance energy in the H−X bond, which

(30) Shaik, S.; Shurki, A. *Angew. Chem., Int. Ed.* **1999**, *38*, 586.
(31) (a) Fox, G. L.; Schlegel, H. B. *J. Phys. Chem.* **1992**, *96*, 298. (b) Hrovat, D. A.; Borden, W. T. *J. Am. Chem. Soc.* **1994**, *116*, 6459. (c) Donahue, M. N.; Clarke, J. S.; Anderson, J. G. *J. Phys. Chem. A* **1998**, *102*, 3923. (d) Clarke, J. S.; Rypkema, H. A.; Kroll, J. H.; Donahue, M. N.; Anderson, J. G. *J. Phys. Chem. A* **2000**, *104*, 4458.

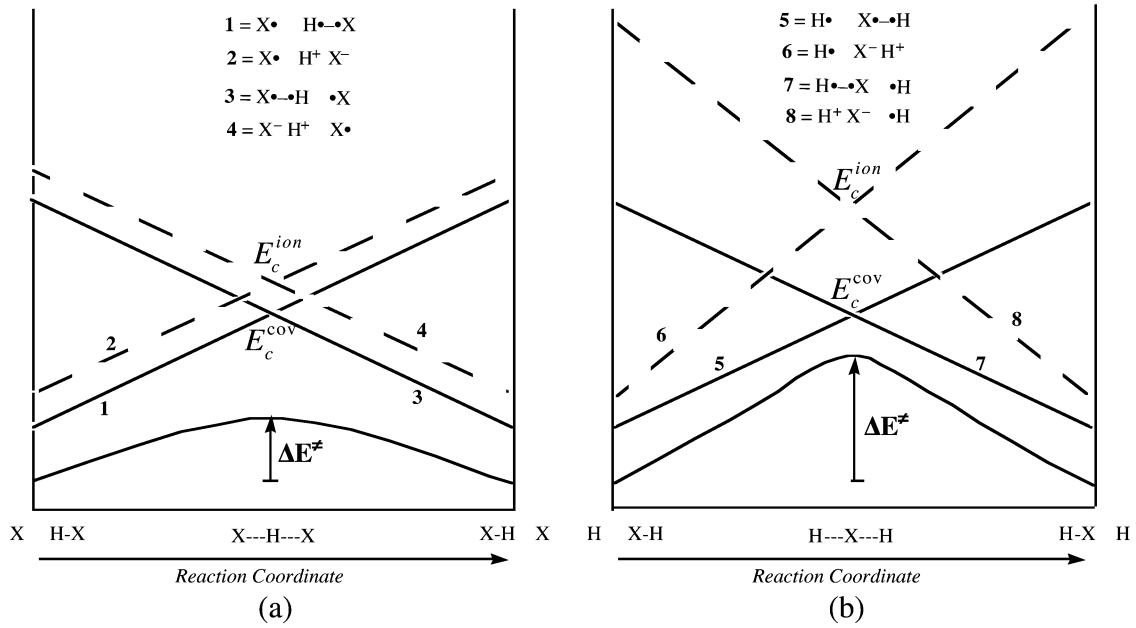

Figure 1. Qualitative VBCMD curve-crossing VB diagrams for (a) the hydrogen exchange reaction, eq 1, and (b) the halogen exchange reaction, eq 2.

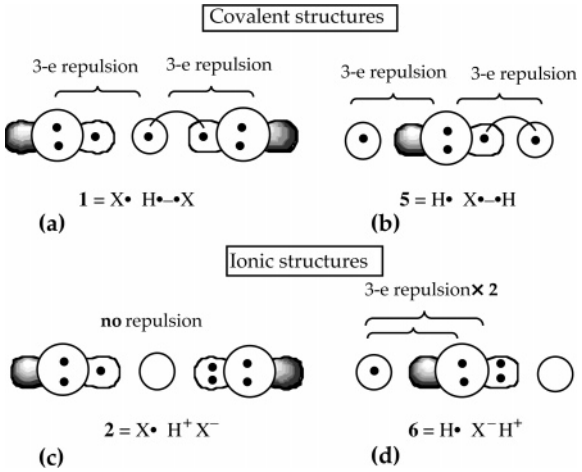

Figure 2. Pauli repulsions taking place in the transition states of reactions 1 and 2. (a) Covalent structure of reaction 1; (b) covalent structure of reaction 2; (c) ionic structure of reaction 1; (d) ionic structure of reaction 2. Mirror-image structures, not shown here, undergo the same Pauli repulsions.

is common to the two reaction types: *the larger the resonance energy in H−X, the larger the loss of resonance energy in reaction 2 with respect to reaction 1, and the larger becomes the barrier difference*. This is where the concept of CS-bonding comes into play.

3. Charge-Shift Bonding

It has been shown in previous papers[6,7] that alongside the classical categories of two-electron bonds (such as the covalent bond that owes its strength to spin-pairing or the ionic bond that is stabilized by electrostatic interactions between the two ions) there exists an additional class of bonds in which the fluctuation of electron pair density, and hence the covalent−ionic resonance energy, plays the dominant role. That is, neither the covalent nor the ionic interactions are responsible, by themselves, for a significant part of the bonding energy, but *the* major cause of bonding is the resonance energy that arises from the mixing of the covalent and ionic components of the bonds. In extreme cases, such as F_2, the covalent interaction is repulsive for any and all F- - -F distances, and this repulsion is more than compensated by the covalent−ionic resonance energy that becomes the only source of binding. This type of bonding, which is associated with charge shift from the covalent to the ionic components, has been called by us "charge-shift" bonding (CS-bonding). It has been recently characterized independently by VB theory and by the theory of electron-localization function (ELF) and was found in homopolar as well as heteropolar bonds.[6,7] Atoms (fragments) that are prone to CS-bonding are typically compact electronegative and/or lone-pair-rich species. As such, the importance of CS-bonding peaks for fluorine, which is the most compact and lone-pair-rich atom in its period. Thus, the F−F but also the H−F bonds are typical CS-bonds, displaying very large covalent−ionic resonance energies, RE_{C-I}.

Turning back to reactions 1 and 2, H−F is a CS-bond while H−Cl and H−Br are classical covalent bonds and have small covalent−ionic resonance energies that decrease from Cl to Br. Thus, qualitative VB theory of reactivity and bonding, and specifically CS-bonding, predicts that HXH barriers will be larger than XHX barriers, in all cases, but that the effect will be particularly large for X = F and less and less important for X = Cl, Br, etc. While these predictions nicely fit the actual situation, there remain quantitative calculations to ascertain that VB theory makes the right predictions for the right reasons.

4. Theoretical Methods

The VB computations are performed by means of the breathing-orbital valence bond method (BOVB). This is an ab initio method that uses nonorthogonal valence bond-type wave function and has been devised to combine the properties of the interpretability and extreme compactness of the wave function, along with reasonable accuracy.[32] In this method, the structural coefficients and orbitals of the VB

(32) For the leading BOVB references, see: (a) Hiberty, P. C.; Flament, J. P.; Noizet, E. *Chem. Phys. Lett.* **1992**, 189, 259. (b) Hiberty, P. C.; Humbel, S.; Byrman, C. P.; van Lenthe, J. H. *J. Chem. Phys.* **1994**, *101*, 5969. (c) Hiberty, P. C. In *Modern Electronic Structure Theory and Applications in Organic Chemistry*; Davidson, E. R., Ed.; World Scientific: River Edge, New York, 1997; pp 289−367. (d) Hiberty, P. C.; Shaik, S. In *Valence Bond Theory*; Cooper, D. L., Ed.; Elsevier: Amsterdam, 2002; pp 187−226. (e) Hiberty, P. C.; Shaik, S. *Theor. Chem. Acc.* **2002,** *108*, 255.

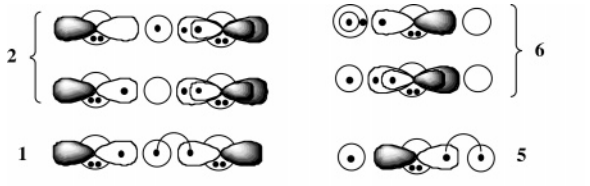

(a) X..H..X complex, reaction (1) (b) H..X..H complex, reaction (2)

Figure 3. Schematic orbital representations of VB structures for the XHX complex (**1**, **2**) and the HXH complex (**5**, **6**). Structures **3**, **4**, **7**, **8** are mirror-image structures of **1**, **2**, **5**, **6**, respectively. For all ionic structures, both spin-couplings are included in the calculations.

structures are optimized simultaneously, while dynamic correlation is introduced by allowing the orbitals to assume sizes and shapes that are different for the different structures.

Among the electrons and orbitals, one distinguishes between an active space, made of the orbitals and the electrons that are directly involved in the bond breaking/forming, and an inactive space, where the orbitals keep the same occupancy throughout the reaction coordinate. The active space is treated at the VB level, and its electrons are explicitly correlated, whereas the inactive part of the molecule is described by a set of doubly occupied orbitals, which are optimized but not correlated. In this manner, the correlation of inactive electrons and the active−inactive correlation are not calculated explicitly. For example, the active orbitals of the H−X molecule are the 1s(H) orbital of the hydrogen atom and the np_z(X) orbital of the halogen. Note that the np_z(X) and ns(X) orbitals are allowed to hybridize freely during the orbital optimization process, albeit such hybridization is normally weak in halogens, especially in fluorine. The same orbitals form the active orbital space of the HXH and XHX species, leading to an active space of three electrons in three orbitals.

The BOVB wave function is composed of a set of VB structures that forms a complete and minimal set (also called Rumer basis) for the description of a given electronic state. For the HXH and XHX complexes, the complete Rumer set is composed of all the linearly independent possible arrangements of three electrons in three orbitals, i.e., two covalent structures and six ionic structures. For the XHX system, this corresponds to the major structures **1**−**4** (Scheme 1) plus some less important structures: X• H$^-$ F$^+$, F$^+$H$^-$ X•, F$^-$ H• F$^+$, and F$^+$ H• F$^-$. Among these extra VB structures the first two are neglected for two reasons: (i) they must be rather minor, owing to the large ionization potential of halogens, and (ii) more importantly, these structures belong to the Rumer sets of the reactants, transition state, and products, so that their neglect leads to quasi-constant errors throughout the reaction coordinate. On the other hand, the last two structures belong to the transition state alone and therefore cannot be neglected without affecting the calculated barriers. For convenience, the minor structures F$^+$ H• F$^-$ and F$^-$ H• F$^+$ will be combined with the major structures **2** and **4**, respectively, in the discussions of the computational results (see Figure 3). Similarly, the major structures **6** and **8** in the HXH system will be complemented by the minor structures H$^-$ F• H$^+$ and H$^+$ F• H$^-$.

The BOVB method has a few levels that differ in hierarchy of sophistication. Here we use an intermediate level, referred to as SL-BOVB, as a compromise between accuracy and simplicity. Relative to the basic level, SL-BOVB splits the active doubly occupied orbital of an ionic structure into two singlet-coupled singly occupied orbitals, as illustrated in Figure 3. This improvement brings some radial correlation to the active electrons. In addition, since now the ionic VB structures possess three singly occupied orbitals, which corresponds to two possible linearly independent spin-eigenfunctions, both spin couplings are included in the calculations. In the HXH system, the inactive lone pairs are allowed to delocalize over the attacking hydrogen, to more accurately describe the three-electron repulsions. Similarly, in the XHX system, the π lone pairs are allowed to delocalize over the two X moieties, to mitigate the repulsions between lone pairs. On the other hand, the orbitals that are involved in a bond are kept strictly localized, so as to keep the distinction between covalent and ionic bonds perfectly clear. All the VB structures that are relevant to this work are those illustrated in Figure 3, together with their mirror-image structures.

Table 1. Transition State Properties for the HXH and HXH Systems, as Calculated by Standard ab Initio Methods[a]

	R (Å)[b]	$\Delta E^{\ddagger}$ (MP2)	$\Delta E^{\ddagger}$ (CCSD(T))	$\Delta\Delta E^{\ddagger}$ (MP2)[b]	$\Delta\Delta E^{\ddagger}$ (CCSD(T))[c]
FHF	1.082	25.3	20.9		
ClHCl	1.470	17.2	11.0		
BrHBr	1.619	12.7	8.0		
HFH	1.129	46.6	42.5	21.3	21.6
HClH	1.469	29.9	18.5	12.7	7.5
HBrHr	1.609	22.7	12.9	10.0	4.9

[a] Energies are expressed in kcal/mol, relative to the reactants. [b] Distances optimized at the MP2 level. [c] HXH vs XHX barrier differentiations, eq 4.

In very large basis sets, using high-rank polarization functions, an optimized atomic orbital may become so distorted that its localization on a given atom becomes meaningless. For this reason, we customarily perform VB calculations using basis sets no larger than double-ζ plus polarization, augmented with diffuse functions when necessary. In accord, the VB calculations in this study were performed using the standard 6-31++G(d,p) basis set.

To assess the accuracy of the VB calculations, two kinds of standard ab initio calculations have been performed: (i) some geometry optimizations and calculations of barriers at the UMP2 level of calculation (second-order Møller−Plesset perturbation theory in its spin-unrestricted formalism). At this level, the maximum spin contamination yielded a value of 0.782 for the mean value of S^2, to be compared with the value 0.75 that is expected for a pure doublet state. (ii) Some single-point calculations at the RCCSD(T) level (coupled cluster calculations in the spin-restricted formalism). These latter calculations use the geometries previously optimized at the UMP2/6-31++G(d,p) level and are performed in the 6-31++G(3df,3pd) basis set.

For the sake of simplicity, all reactions are studied in their collinear forms. This simplification is enabled because in the cases studied here the bent transition-state structures are only slightly lower in energy than the linear ones, and the trends in a given XHX series are conserved in the linear structures as in their bent counterparts.

The Gaussian 98 series of programs[33] was employed for all calculations of Møller−Plesset and RCCSD(T) types. The MOLPRO package has been used for the RCCSD(T) calculations.[34] The ab initio valence bond calculations were performed with the XMVB program.[35]

5. Computational Results

5.1. Standard ab Initio Calculations. Two kinds of standard ab initio calculations were performed on reactions 1 and 2: (i) a simple MP2 calculation in 6-31++G(d,p) basis set, to verify that the tendencies that we are going to explain are still apparent at modest levels of calculation, and (ii) some higher-level calculations at the RCCSD(T)/6-31++G(3df,3dp) level, to get a uniform set of barriers for both reactions at a fairly accurate level. The results are displayed in Table 1.

Table 1 shows the MP2/6-31++G(d,p) optimized bond lengths, for the H−X reactants and the transition states of both reactions. As expected, bond lengths in the transition states

(33) Frisch, M. J.; et al. *GAUSSIAN 98*; Gaussian, Inc.: Pittsburgh, PA, 1998.
(34) MOLPRO is a package of ab initio programs written by H.-J. Werner and P. J. Knowles, with contributions from R. D. Amos, A. Bernhardsson, A. Berning, P. Celani, D. L. Cooper, M. J. O. Deegan, A. J. Dobbyn, F. Eckert, C. Hampel, G. Hetzer, T. Korona, R. Lindh, A. W. Lloyd, S. J. McNicholas, F. R. Manby, W. Meyer, M. E. Mura, A. Nicklass, P. Palmieri, R. Pitzer, G. Rauhut, M. Schütz, H. Stoll, A. J. Stone, R. Tarroni, and T. Thorsteinsson.
(35) Song, L.; Wu, W.; Mo, Y.; Zhang, Q. *XMVB-01*: An ab initio Non-orthogonal Valence Bond Program; Xiamen University: Xiamen 361005, China, 2003.

Table 2. Properties of the H−X Molecules, as Calculated at the BOVB Level[a]

	R (Å)	D_e (full-BOVB)[b]	D_e (covalent)[c]	RE_{C-I}[d]
FH	0.926	122.9	35.4	87.5
ClH	1.303	88.8	58.5	30.3
BrH	1.440	75.4	57.1	18.3

[a] Energies in kcal/mol, relative to the separate atoms. [b] Both covalent and ionic structures included. [c] Wave function restricted to the covalent structure. [d] Covalent−ionic resonance energies.

increase in the series X = F to Br, in the same order as for the H−X bond lengths in the reactants. However, the bond lengths are roughly the same in the HXH and XHX transition states for X = Cl and Br. By contrast, the HFH transition state is significantly more elongated than FHF, in accord with the very large barrier difference between the corresponding reactions. Curiously, for X = Cl or Br, the HXH transition states are even slightly tighter than the XHX ones, in apparent disagreement with the barrier ordering (HXH > XHX). This subtle, but counterintuitive effect can be understood to be a consequence of the repulsions between the lone pairs of the two halogen atoms in XHX, an effect that we have not considered up to now and that will become apparent soon.

At both computational levels, MP2 and RCCSD(T), the calculated barriers in Table 1 reproduce the tendencies that motivated this work: (i) In both reactions 1 and 2, the barriers decrease in the series X = F, Cl, and Br, and (ii) in all cases, the HXH barriers are higher than the corresponding XHX ones, and the barrier difference, $\Delta\Delta E^{\ddagger}$ in eq 4, decreases as we progress from X = F to X = Br.

$$\Delta\Delta E^{\ddagger}(\mathrm{HXH-XHX}) = \Delta E^{\ddagger}(\mathrm{HXH}) - \Delta E^{\ddagger}(\mathrm{XHX}) \quad (4)$$

The barrier differences show some dependence on the level of calculation. At the MP2 level, these barrier differences are 21.3, 12.7, and 10.0 kcal/mol, respectively, for the series X = F, Cl, Br. However, while the $\Delta\Delta E^{\ddagger}$ value is about the same at the RCCSD(T) level for X = F, much smaller barrier differences are found for X = Cl and Br, respectively 7.5 and 4.9 kcal/mol. Thus, the accurate level makes a clear-cut difference between the reactions involving fluorine on one hand, and those involving chlorine or bromine on the other hand.

5.2. Valence Bond Calculations. Table 2 reports the BOVB-calculated bond lengths and dissociation energies for the H−X bonds, at a level consistent with the rest of this study (neglecting the $H-X^+$ structures). Also reported are some additional VB quantities; the dissociation energies calculated at the purely covalent level (only keeping the H•−•X VB structure in the calculation) and the ionic−covalent resonance energies.

It is immediately apparent that the covalent interaction accounts for a significant part of the bonding energy for H−Cl and H−Br, respectively 66% and 76% of the total bond energy. On the other hand, the situation is fundamentally different for the H−F bond. Here the covalent interaction represents only 29% of the bonding energy, while the huge resonance energy of 87 kcal/mol becomes the major effect responsible for bonding. According to our classification, the H−F bond belongs to the category of "charge-shift" bonds, while H−Cl and H−Br are ordinary polar covalent bonds.[6,7]

The BOVB calculations for the XHX and HXH transition states are displayed in Table 3. As already noted for radical species,[32c] the BOVB-optimized bond lengths are found to be consistently longer than the UMP2-optimized ones, while intermediate values are generally found with more accurate methods. Very probably, this comes from the fact that our BOVB method does not use the spin-unrestricted formalism.

Table 3. Transition State Properties for the HXH and HXH Systems, as Calculated by the BOVB Method[a]

	R (Å)	$\Delta E^{\ddagger}$ (full-BOVB)[a]	$\Delta E^{\ddagger}_{cov}$[c]	RE_{C-I}[d]
FHF	1.1105	22.4	56.6	121.7
ClHCl	1.5357	19.2	35.2	46.9
BrHBr	1.6720	8.3	29.6	39.6
HFH	1.1759	46.6	52.0	92.9
HClH	1.5455	24.1	32.1	38.9
HBrH	1.6695	14.7	24.6	28.2

[a] Energies in kcal/mol, relative to the reactants. [b] Both covalent and ionic structures included. [c] Wave function restricted to the covalent structures. [d] Covalent−ionic resonance energies.

Table 4. BOVB Calculated Transition State Properties for the XHX and HXH Systems, Restricted to the Covalent Structures[a]

	R (Å)	$\Delta E^{\ddagger}_{cov}$
FHF	1.743	38.2
ClHCl	1.662	32.5
BrHBr	1.787	27.4
HFH	1.855	38.6
HClH	1.637	31.3
HBrH	1.731	24.1

[a] Energies in kcal/mol, relative to the reactants.

With the unique exception of ClHCl, the other BOVB-calculated $\Delta E^{\ddagger}$ barriers for reactions 1 and 2 lie between the UMP2 and RCCSD(T) values. Thus, the accuracy of our BOVB barriers is only fair, which is not surprising, owing to the nature of the transition states that are the sites of more numerous Pauli repulsions, which would necessitate large basis sets and higher levels of correlation to be accurately taken into account. However, what matters is that the (HXH−XHX) barrier difference, $\Delta\Delta E^{\ddagger}$ (eq 4), is well reproduced at the BOVB level, and the error relative to the $\Delta\Delta E^{\ddagger}$ at the RCCSD(T) level does not exceed 2.6 kcal/mol. Thus, just like the accurate MO-based level, the BOVB calculation makes a clear-cut distinction between the (X = F) case, where the HXH barrier is much larger than the XHX one and the two other cases (X = Cl, Br) where this difference is much smaller. It is therefore meaningful to pursue the analysis of barrier formation at the BOVB level.

Let us now examine the effect of removing the ionic components from the VB wave functions and re-optimizing the covalent component, without changing the HX bond lengths of the transition states and reactants (Table 3, column 4). All the so-calculated covalent barriers, $\Delta E^{\ddagger}_{cov}$, are significantly higher than the true barriers $\Delta E^{\ddagger}$, a simple consequence of the fact that the covalent wave functions are not in their own optimized geometries. The covalent barriers are much higher in the fluorine case than in the chlorine or bromine case, but the most remarkable fact is that, in each case, the XHX barriers are quite close to the HXH ones; this tendency is confirmed by more refined calculations, in which the covalent structures of both the HX reactants and the transition states are considered at their own optimized geometries (Table 4). It first appears that when X = F the geometries of the HXH and XHX transition states are extremely loose, with H−F distances being around 1.8 Å, and *get tighter* for X = Cl. This startling result is a direct consequence of the charge-shift-bond character of the H−F

bond: in the absence of covalent−ionic resonance energy, the covalent interaction, by itself, has a very weak bonding capability (see Table 2), and hence the loose geometry. On the other hand, since the H−Cl and H−Br bonds are not CS-bonds, the optimized geometries of the covalent-components of the corresponding transition states are not so much elongated compared with the full-BOVB geometries that are obtained with inclusion of ionic structures.

The most remarkable result that emerges from Table 4 is the great similarity between the covalent barriers for XHX vs HXH. For X = F, the barriers are almost exactly the same, in perfect agreement with the predictions of the qualitative VB model above. For X = Cl or Br, the XHX barrier is even slightly higher than the HXH one, meaning that the electronic effects that are present in the covalent wave function lead to an HXH/XHX barrier differentiation that is not only small but even varying in the wrong way.

The results of the covalent-only VB calculations indicate that the HXH vs XHX barrier differences are entirely due to the mixing of the ionic structures, through the difference in the covalent−ionic resonance energies, RE_{C-I}. These quantities are shown in the last column of Table 3. As a rule, the RE_{C-I} values are consistently larger for the transition states than for the H−X molecules. This is not surprising, since the transition state is the site of the mixing of four VB structures, vs only two for the H−X reactant. However, the most interesting result is that the resonance energies are always significantly larger for the HXH than for the XHX transition states. As we recall, this was predicted above by the qualitative VB model, and shown to derive from the destabilization of the ionic VB structures in the HXH case. Moreover, if we compare the HXH vs XHX transition states, there is a quantitative correspondence between the RE_{C-I} differences and the barrier differences: 28.8 kcal/mol vs 24.2 (X = F), 8.0 vs 4.9 and 11.4 vs 6.4 for the other two cases.

6. Discussion

According to the qualitative VB analysis, the condition for the HXH barrier to be higher than XHX at the covalent level is a significant hybridization of the *n*s lone pair of the halogen atom in structures **1** and **3** of HXH. The above results clearly show that this effect is not significant since the covalent barriers of XHX vs HXH are hardly different; in fact, the XHX covalent barriers are the largest ones in the cases of X = Cl and Br. In these latter cases, it appears that the covalent structures of XHX undergo, in fact, slightly *more* repulsions than the corresponding VB structures of HXH. This can be readily attributed to an effect that we have neglected up to now in the qualitative analyses, the mutual left−right repulsions between the lone pairs of the halogen atoms that face each other in XHX. This effect manifests for X = Cl or Br but is very small in the fluorine case, owing to the long H−F distance and the compactness of the fluorine atoms.

It follows from the above that the barrier differentiation between reactions 1 and 2 cannot arise from Pauli repulsions in the covalent structure, due to the interaction between the *n*s halogen lone pair with the neighboring hydrogens in HXH, as formerly proposed.[19,28,29] Rather, this difference must be entirely ascribed to the effect of ionic structures, through the RE_{C-I} resonance energies of the HXH and XHX transition states and their difference ΔRE_{C-I} (eq 3). This latter quantity becomes increasingly more important as the covalent−ionic resonance energy of the X−H bond of the reactant gets larger, and the HXH vs XHX barrier differentiation follows the same tendencies. Thus, as the resonance energy diminishes in H−X when X changes from F to I (a clear tendency even if we did not include iodine in the present calculations), the barrier difference also diminishes in the same series (X = F to I). This correlation between the two quantities proves to be more than a mere logical relationship. In fact, the two quantities are actually related by a proportionality factor. Thus, using the covalent−ionic resonance energies of H−X reactants (Table 2) we may calculate the barrier differences simply as follows:

$$\Delta\Delta E^{\ddagger} = 0.25\ RE_{C-I}\,(H-X) \qquad (5)$$

This remarkably simple relationship predicts the following barrier differences 21.9, 7.6, and 4.6 kcal/mol in the series (X = F, Cl, Br), in very good agreement with the accurately calculated values (21.6, 7.5, and 4.9, Table 1, last column). *It follows therefore that, the barrier differences between the H transfer and halogen transfer reactions is a sensitive measure of the covalent−ionic resonance energy in the H−X bond.*

7. Conclusion

The barrier differences between hydrogen exchange, reaction 1, and the corresponding halogen exchange processes, reaction 2, were elucidated in this study by means of ab initio calculations using the breathing-orbital valence bond method. These calculations show that covalent VB structures play no role in this barrier differentiation, which rules out some formerly proposed explanations in terms of Pauli repulsions between the *n*s lone pair of halogen and the neighboring hydrogens in the HXH system. On the other hand, the mixing of the ionic VB structures into the covalent structures is entirely responsible for the barrier differentiation. As shown by a qualitative analysis that is further confirmed by quantitative calculations, the ionic structures of the HXH transition state are destabilized relative to those of the XHX system. Consequently, the ionic structures of HXH transition state mix to a lesser extent with the covalent structure, compared with the XHX transition states. As such, the loss of covalent−ionic resonance energy in the HXH transition states accounts fully for the excess barrier for halogen transfer compared with hydrogen transfer.

More importantly, the barrier difference can be quantified by the simple expression in eq 5, as one-quarter of the covalent ionic resonance energy of the H−X bond. As such, the present study shows that the relative barrier for HXH vs XHX *is an experimental measure of the covalent−ionic resonance energy arising from the mixing of covalent and ionic structures in the polar H−X bond that undergoes cleavage and remaking during the two processes*. This resonance energy quantity, which has long been used as a model-dependent and rather heuristic concept, is given here a strong link to experiment. Thus, in the same way as resonance between two Kekulé structures, e.g. in benzene, is associated with some thermodynamic stability, the covalent−ionic resonance energy in a polar bond appears as a meaningful chemical quantity that can be experimentally probed.

An outcome of this link between theory and experiment is the confirmation of the special status of the H−F bond. This bond is shown, in this study and in others,[6] to display a

particularly large covalent−ionic resonance energy, to the extent that this latter quantity constitutes the major cause for bonding. Bonds belonging to this category have been termed "charge-shift" bonds. Charge-shift bonding was recently shown to manifest, beyond VB theory, by peculiar electron density maps in the ELF/DFT framework.[7] It follows from the above study that the very large barrier in the HFH reaction is nothing else but a consequence of the charge-shift character of the H−F bond, while the H−Cl and H−Br bonds are ordinary polar covalent bonds and require much lower barriers for the halogen exchanges. *This charge-shift character is now shown to manifest itself by an experimentally measurable and chemically important quantity such as activation energy*. Research is continuing in our groups to trace other experimental manifestations of CS-bonding, which we believe to have a large territory.

Acknowledgment. The research at XMU was supported by the National Science Foundation and the Basic Research Program of China. The research by Shaik was supported by the German Federal Ministry of Education and Research (BMBF) within the framework of the German-Israeli Project Cooperation (DIP).

Supporting Information Available: Complete ref 33. This material is available free of charge via the Internet at http://pubs.acs.org.

JA053130M